Primary Wave Energy Conversions of Oscillating Water Columns

Wanan Sheng[#1], Raymond Alcorn [#2], Anthony Lewis [#3]

[#]*Beaufort Research-HMRC, University College Cork*
Youngline Industrial Estate, Pouladuff Road, Cork, Ireland

[1]w.sheng@ucc.ie

[2]r.alcorn@ucc.ie

[3]t.lewis@ucc.ie

***Abstract*—This paper presents a study on the numerical simulation of the primary wave energy conversion in the oscillating water column (OWC) wave energy converters (WECs). The new proposed numerical approach consists of three major components: potential flow analysis for the conventional hydrodynamic parameters, such as added mass, damping coefficients, restoring force coefficients and wave excitations; the thermodynamic analysis of the air in the air chamber, which is under the assumptions of the given power take-off characteristics and an isentropic process of air flow. In the formulation, the air compressibility and its effects have been included; and a time-domain analysis by combining the linear potential flow and the thermodynamics of the air flow in the chamber, in which the hydrodynamics and thermodynamics/aerodynamics have been coupled together by the force generated by the pressurised and de-pressurised air in the air chamber, which in turn has effects on the motions of the structure and the internal water surface. As an example, the new developed approach has been applied to a fixed OWC device. The comparisons of the measured data and the simulation results show the new method is very capable of predicting the performance of the OWC devices.**

***Keywords*—Wave energy converter, oscillating water column, air compressibility, power take-off**

I. INTRODUCTION

OWC wave energy converters have been, often referred as the first generation of wave energy converters, advanced a great deal since the earliest OWC devices have been studied and widely implemented for powering the navigation buoys since 1940s (see Falcao [1]), and now some practical OWC plants have been built and generated electricity to the grid. It is reported that the LIMPET OWC plant has generated electricity to the grid for more than 60,000 hours in a period of more than 10 years (Heath [2]). A recent development is the Mutriku OWC wave energy plant in Spain [3], a multi-OWC wave energy converters, including 16 sets of "Wells turbines + electrical generator" (18.5 kW each). It is estimated electricity generation of 600 MWh so far [4].

To improve wave energy conversion by the OWC devices, numerical analyses and physical model tests are often used. Earlier theoretical work on the hydrodynamic performance of OWCs has shown that OWC devices could have a high primary wave energy conversion efficiency if the optimized damping can be attained (Sarmento et al [5], Evans [6], Evans and Porter [7]). However, the experimental studies on the bottom-fixed or floating OWCs have shown that the wave energy conversion efficiency of an OWC device very much depends on the damping coefficients of the flow passing through the power take-off system, as well as the size of the water column (water column sectional area and length). Toyota et al. [8] have shown that both the size of the air chamber and the length of the horizontal duct length of a BBDB device have significant effects on the primary power conversion of the OWC wave energy converters. Imai et al.[9] have also studied the influence of the horizontal duct length to the wave energy capture capacity in a BBDB device, and shown that a longer horizontal duct has increased the maximum internal-water-surface (IWS) response to a longer resonance period. As a result of this, a longer horizontal duct may be desirable for tuning the BBDB to the wave states of longer wave periods. Morris-Thomas et al. [10] have experimentally studied the hydrodynamic efficiency on fixed OWCs with different front shapes. From the comparison, it can be seen that the front shapes have some but limited effects on the wave energy conversion efficiencies. For the tested four different front shapes, the wave energy capture

efficiencies are overall similar, and the maximum wave energy conversion efficiency is about 70%.

Another important aspect for the OWC wave energy devices is the air compressibility in the air chamber due to the large space and large pressure in the air chamber. Sarmento et al [11] have proposed a linearized formula for the flowrate through the power take-off system, based on an assumption of an isentropic flow. Sheng et al. [12] have recently formulated a full thermodynamic equation for the air flow in the chamber and through the power take-off system for studying the air compressibility. To validate the air compressibility predicted by the numerical method, a piston connected to a linear test rig, which models an OWC device, can be driven in a much powerful manner so that an obvious air compressibility can be created in the chamber. It is shown that the numerical method has well predicted the compressibility when compared to the experimental data.

In the paper, a new numerical analysis method in the primary wave energy conversion of the OWC devices has been developed and described. The numerical analysis principally consists of following three components:

Frequency domain analysis:

Conventional potential analysis to the hydrodynamics of the OWC device, including the performance of the water column (piston) in frequency domain, and from which the relevant parameters for time-domain are derived; in the frequency domain analysis, a two-body system has been adopted.

Thermodynamic analysis of the air flow in chamber:

The air flow in the chamber is studied under the given characteristics of the PTO system, i.e., the relation between the pressure drop across the PTO and the flow rate through the PTO. The PTO device can be linear, such as the Wells turbine, or nonlinear (e.g., impulse turbine) or a more generic relation using a second-order polynomial function.

Time domain analysis:

Time-domain (TD) equation is established for the dynamics of the water column (piston) for an OWC device by combining the structure of the device (Rigid Body 1) and the water column (the piston, Rigid Body 2). As an example, the OWC device considered here is a fixed OWC which has only one motion mode: heave. In the time domain analysis, the force due to the chamber pressure is included for the piston motion (internal water surface motion).

II. Research on OWC WECs

A. *Numerical approaches*

Potential theory has been widely used to study the OWC devices. For some specific OWC devices, such as two-dimensional OWC devices, or some three-dimensional OWCs with very simple structures, analytical solutions are possible (Evans and Porter [7], Martins-rivas et al [13], Mavrakos et al. [14]), but more popular approaches are the numerical analysis using the well-developed boundary element method, such as WAMIT [15], ANSYS AQWA [16]et al. These commercial codes are readily available for any geometry of interest.

Based on the assumption of the potential flow, the velocity potential of the flow around the floating structure satisfies the Laplace equation:

$$\nabla^2 \varphi = 0 \tag{1}$$

where φ is the frequency-domain velocity potential of the flow around the floating structure (the corresponding time-dependent velocity potential should read $\Phi = \varphi e^{i\omega t}$).

An earth-fixed coordinate system is defined for the potential flow problem. The coordinate is fixed in such a way that the *x*-*y* plane is on the calm water surface and *z*-axis positive up vertically. Its origin coincides with the centre of gravity of the device in calm water. In the coordinate, the free surface conditions can be expressed in frequency domain (see Lee et al. [17]), as

$$\frac{\partial \varphi}{\partial z} - \frac{\omega^2}{g}\varphi = \begin{cases} 0, & (on\ S_f) \\ -\dfrac{i\omega}{\rho g} p_0, & (on\ S_i) \end{cases} \tag{2}$$

where ω is the wave frequency, ρ the density of water, g the acceleration of gravity, p_0 the pressure amplitude acting on the interior water surface, S_i the interior water surface in the water column, and S_f the free surface but excludes the interior free surface.

To solve the hydrodynamic problem, two different approaches can be used: massless piston model [17, 18]and pressure distribution model (Evans et al. [19]). In the former approach, the internal free surface is assumed to behave as a massless rigid piston. In the latter approach, the internal free-surface condition and the spatial variation of the internal free surface is represented in terms of the dynamic air pressure in the chamber.

In this research, the first approach is applied. To include the interior water surface as a boundary in the conventional BEM code WAMIT [15], Lee et al.[20] introduced the so-called generalized modes for the interior water surface motions, such as the piston-type and the first sloshing modes of the interior water motions so that the response of the interior water surface can be obtained in WAMIT without significant modifications to the code. Following this principle, the numerical simulations in this research are all conducted using WAMIT.

B. *Experimental investigations*

For OWC devices, the air passing through the PTO system is a reciprocating process during a wave period. To convert

the pneumatic power into mechanical power, different design strategies for the power take-off have been proposed, but the most popular types of the pneumatic power conversion are the air turbines, such as the Wells turbine [21-23], impulse turbine [24-26], and the self-pitch controlled air turbine [27] et al. A review on the air turbines for wave energy conversion has been recently given by Takao et al. [28].

The Wells turbine is well known to have a linear damping relation between the pressure drop across the PTO and the flowrate, and their relation can be expressed as

$$p = k_1 Q_p \tag{3}$$

where p is the chamber pressure, Q_p the airflow through the power take-off system, and k_1 the damping coefficient.

For impulse turbines, the nonlinear relation between the chamber pressure and the flowrate can be approximated by the following expression as,

$$p = k_2 |Q_p| Q_p \tag{4}$$

where k_2 is the nonlinear damping coefficient.

In small scale OWC model tests, the PTO systems (air turbines) have been supposed to be scaled for testing according to the relevant similitude laws, the size and the damping characteristics and so on. However, it is practically difficult to manufacture a small scaled air turbine which maintains the correct characteristics of the air turbines, due to the large frictions in the scaled power take-off system (Payne [29]). Alternatively, it is more practical to model the relation between the chamber pressure and flowrate, for example, the linear relation of the PTO system can be modeled by porous membrane (see Lewis et al.[30] and Forestier et al.[31]), while the nonlinear relation has been widely modelled by orifice plates [8-10, 32, 33]. It is shown if the orifice ratio (defined as the orifice area divided by water column area) is between 0.5%-2.0%, the corresponding damping levels will give the OWC devices an optimal wave power conversion efficiency.

III. Performance of OWC devices

As an example, a generic cylinder OWC is studied. Figure 1 shows a generic bottom-fixed OWC which is fixed on a fixed frame on the tank floor. This fixed OWC model is well isolated from the influence of the ambient structures. The generic OWC has a water column of a diameter of 0.104m, a draught of 0.3m, and a wall of thickness of 0.106m. The details of the model can be found in Sheng et al. [34].

To measure the wave power extracted by the OWC device, a pressure transducer is mounted on the top of the water column. In addition, the motion of the interior water surface is also measured by a float which supports a marker. In principle, the power can be calculated by the pressure drop across the orifice and the flowrate passing the orifice. Due to the well-established relation between the flowrate and the chamber pressure, the extracted power can be calculated either by the chamber pressure only or by the motion of the interior water surface (from which the flowrate can be easily calculated).

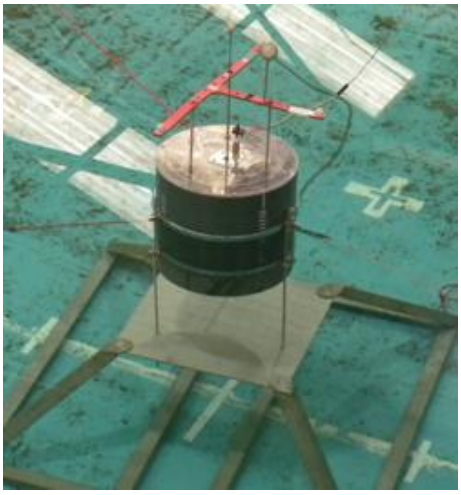

Figure 1 Fixed cylindrical OWC tested in HMRC ocean wave tank

In the numerical study, the internal water surface (IWS) response is predicted as large as 26 (see Figure 2) if no viscous damping coefficient has been included. The added viscous damping brings down the IWS response greatly to 7. It must be noted that the added viscous damping is purely induced by the motions of the structure and the water column, where the damping from the PTO system is not included. For example, in the experiment, an orifice of 12mm diameter has been installed on the top of the OWC device, the measured IWS response is given in Figure 3. Principally, the measured IWS response has included all dampings, such as hydrodynamic damping, viscous damping and the damping from the PTO. The comparison in Figure 3 shows the difference between the IWS responses with and without PTO damping, where the numerical prediction is without PTO damping. The numerical prediction with PTO will be dealt with later in the report.

IV. Effects of air compressibility

As pointed out by Sarmento et al. [5], the spring-like effect of the air compressibility in the air chamber can not be negligible for the full scale OWC devices in which the air chamber may be large enough. In addition, for the full scale OWC devices, the chamber (gauge) pressure and its gradient with regard to time can be large enough to create compressibility in the air chamber. Sarmento et al. [35] give a linearized formula for calculating the air flow through the power take-off device as,

$$Q_p = Q_w - \frac{V_0}{\gamma p_0}\frac{dp}{dt} \tag{5}$$

with Q_p and Q_w being the flowrate through PTO and driven by water free surface, V_0 the undisturbed volume of the air, p_0 and p the atmospheric pressure and the chamber pressure, γ the special heat ratio of air (γ=1.4 for air).

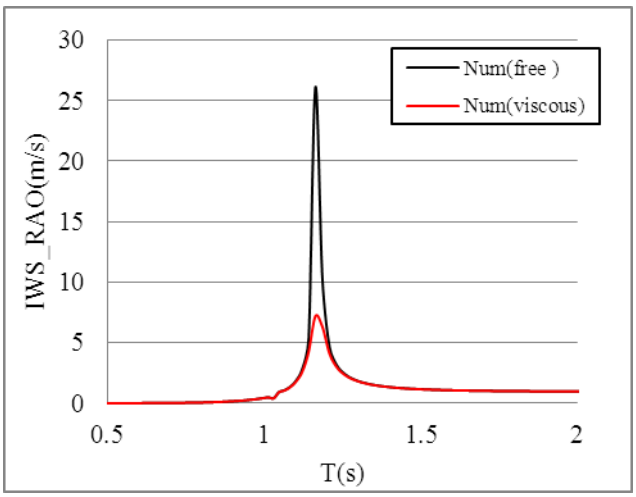

Figure 2 Numerical predictions of the IWS motion responses of a fixed OWC (without and with added viscous damping)

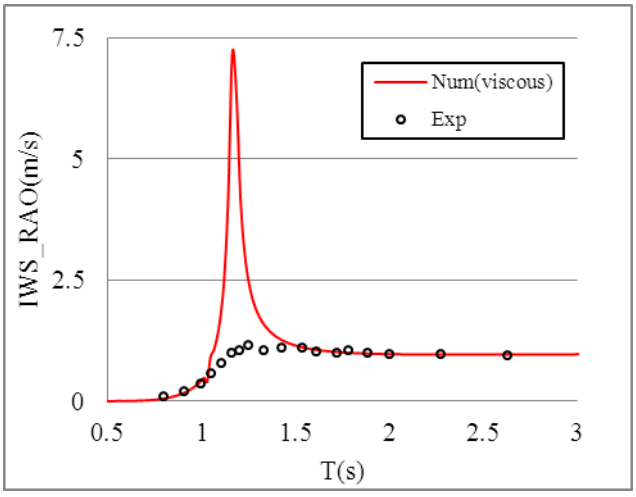

Figure 3 IWS responses of a fixed OWC: numerical response against the experimental data with an orifice φ=12mm

Based on the flowrate formula, the power available to the PTO, P_p, and the input power provided by the water free surface, P_w, are calculated as,

$$\begin{cases} P_p = p \times Q_p \\ P_w = p \times Q_w \end{cases} \tag{6}$$

Due to compressibility of the air, the instantaneous flowrates driven by the interior water surface and through the PTO may be different. Hence, the instantaneous input power P_w and the power through the PTO, P_p, may be different. A numerical study conducted by Thakker et al. [36] has indicated that the air compressibility may reduce the efficiency of the air chamber by about 8%. This following analysis will address the compressibility problem, and check the possible reduction of the efficiency of the air chamber due to compressibility, via both experimental data and numerical prediction.

A. *Thermodynamics of air flow*

For studying the air compressibility of the air, Sheng et al. [12] have proposed a method to predict the air compressibility in the air chamber based on the known PTO characteristics and an isentropic process of the air in the chamber. For completeness, the method is outlined here.

The mass of air enclosed in the air chamber can be expressed as

$$m = \rho_c V \tag{7}$$

where m is the time dependent air mass in the air chamber, V the air volume of the air chamber, ρ_c the air density in the chamber.

Differentiating eq. **(7)** yields,

$$\frac{dm}{dt} = \rho_c \frac{dV}{dt} + V \frac{d\rho_c}{dt} \tag{8}$$

It is noted that a positive value of the mass rate with regard to time means some air is inhaled in through the PTO system (mass increase), and a negative value of the mass rate means some air is driven out of the air chamber (mass reduction).

Due to the air compressibility, the air density changes in the air chamber in exhalation and inhalation. For pressurized chamber, the air is pressured to have a higher density (than that of atmosphere) and is driven out of the air chamber through the power take-off system. In inhalation, the chamber is de-pressurized, and atmosphere is inhaled into the chamber through the power take-off system. Obviously, the air flow through the PTO system with different density must be considered for exhalation and inhalation separately.

Exhalation:

$$Q_p = -\frac{1}{\rho_c}\frac{dm}{dt} \tag{9}$$

Inhalation:

$$Q_p = -\frac{1}{\rho_0}\frac{dm}{dt} \tag{10}$$

where ρ_0 is the atmospheric density, and a positive flowrate Q_p through the PTO means the flow exhaled from the air chamber.

Following many other researchers for this topic, the analysis is simplified: the air in the chamber is assumed as isentropic process, and under such an assumption, a state equation for the open system is,

$$\frac{p_c}{\rho_c^{\gamma}} = constant \tag{11}$$

which can lead to a linearized form for the density due to the fact of the chamber (gauge) pressure p is normally much smaller than the atmospheric pressure p_0, as

$$\rho_c = \rho_0\left(1+\frac{p}{\gamma p_0}\right) \tag{12}$$

so

$$\frac{d\rho_c}{dt} = \frac{\rho_0}{\gamma p_0}\frac{dp}{dt} \tag{13}$$

Thus for exhalation,

$$Q_p = Q_w - \frac{V}{\gamma p_0 + p}\frac{dp}{dt} \tag{14}$$

Similarly, for inhalation,

$$Q_p = \left(1+\frac{p}{\gamma p_0}\right)Q_w - \frac{V}{\gamma p_0}\frac{dp}{dt} \tag{15}$$

B. *Orifice power take-off system*

In this report, an orifice is the nonlinear PTO for this study. The general relation of the chamber pressure and the flowrate through the PTO is given by Eq. (4). Specifically, for exhalation process, it is

$$p = k_2 Q_p^2 \tag{16}$$

where k_2 is the damping coefficient of the PTO.
It corresponds to

$$Q_p = \sqrt{\frac{p}{k_2}} \tag{17}$$

And for inhalation

$$p = -k_2 Q_p^2 \tag{18}$$

which corresponds to

$$Q_p = -\sqrt{\frac{-p}{k_2}} \tag{19}$$

The flowrate driven by the interior water surface can be expressed as

$$Q_w = -\frac{dV}{dt} \tag{20}$$

Substituting (17) and (20) into (14) yields a dynamic equation for exhalation

$$\frac{dV}{dt} + \frac{V}{\gamma p_0 + p}\frac{dp}{dt} + \sqrt{\frac{p}{k_2}} = 0 \tag{21}$$

Substituting (19) and (20) into (15) yields a dynamic equation for inhalation

$$\left(1+\frac{p}{\gamma p_0}\right)\frac{dV}{dt} + \frac{V}{\gamma p_0}\frac{dp}{dt} - \sqrt{\frac{-p}{k_2}} = 0 \tag{22}$$

V. Experimental validation

By solving equations (21) and (22), we can obtain the air pressure in the chamber based on the known air flow driven by the interior water surface, or we can obtain the chamber air volume based on the known chamber pressure.

To validate the method, an experiment is conducted to simulate an oscillating water column and the power take-off system. In the experiment setup, a well-controlled piston is used to simulate the air chamber and the interior water surface, and on top of the piston, an orifice is installed for simulating a non-linear power take-off (for instance, an impulse turbine), see Figure 4. In this study, the diameter of the piston is 0.3m, and the orifice 0.019m (the ratio of orifice is about 0.004, or 0.4%).

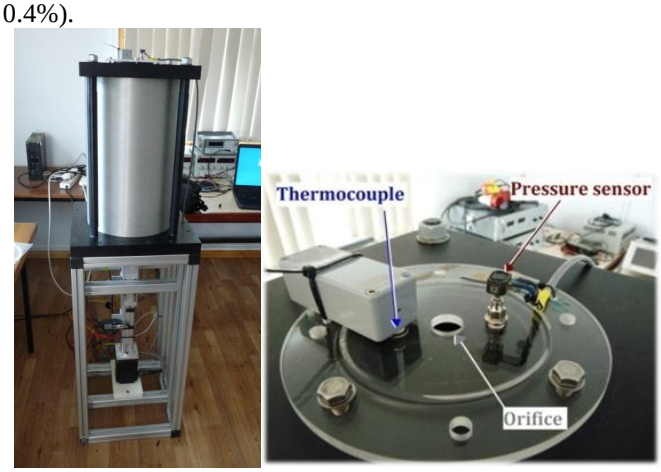

Figure 4 Piston on a test rig (left) and orifice on the top of the piston (right)

In the test, the piston motion, the chamber pressure and the temperature of the air in the chamber are measured. Figure 5 shows the measured data (triangles) for a case of piston amplitude of 0.045m and frequency of 1.0 Hz, and the orifice has a diameter of 0.019m. Under such condition, the power generated in the chamber is up to 80W, which is much more powerful than that we can get in the wave tank test for a same size device. As a result of this, a hysteresis loop between the chamber pressure and the flowrate can be obviously seen (Figure 5), which is a basic feature of the compressible air. To indicate the difference between the incompressible and compressible air, the relation of incompressible air is also plotted (thick solid line in Figure 5).

The numerical prediction of the pressure based on the above theory is also plotted (dashed line in Figure 5). From the comparison, it can be seen that the chamber pressure has been well predicted.

It must be noted that in the figure, some points are apart from the hysteresis loop for both measured data and the predicted data. The reason for this is actually caused by the measurement errors in the measurement of the position of the piston (in the numerical simulation, same piston position is used for both experiment and prediction. If we apply a lower-pass filter to the piston motion (0-12.5Hz frequency band), then the measured and predicted data can be seen in Figure 6, where all the measured and predicted data are very close to the loop. And it is also found that there are some small differences between the measured and predicted data when the pressure returns from its peak.

Figure 7 shows the comparison of measured chamber pressure and the predicted chamber pressure for the case of A=0.045m, f=1.0Hz (ϕ=0.019m). It can be seen that the predicted pressure is in a very good agreement with the measured chamber pressure. Figure 8 shows a comparison of the measured chamber pressure and the predicted pressure in a slower piston motion in which the frequency of the piston motion is 0.5Hz. It can be seen that the case with a smaller frequency has a much smaller air compressibility. Again, the predicted pressure is very close to the measured pressure.

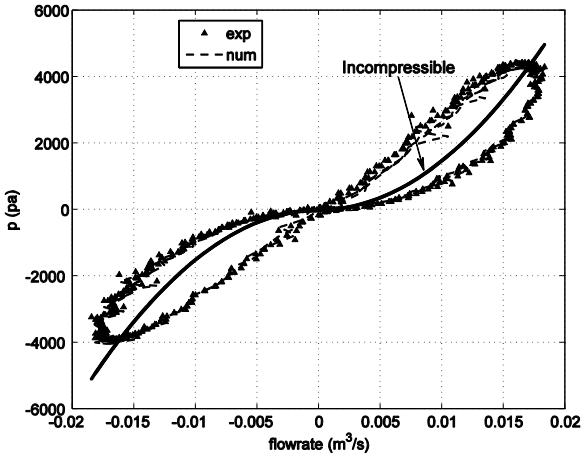

Figure 5 Comparison of measured and predicted pressure-flowrate

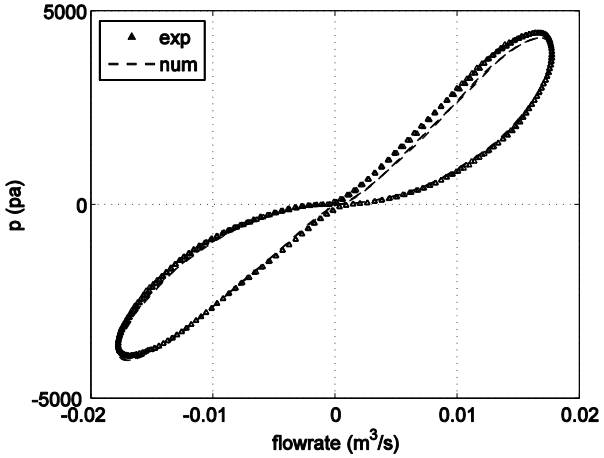

Figure 6 Filter has been applied (components of high frequency are filtered out)

After the solution of the pressure in the air chamber, the input power and the power through the orifice can be calculated by Eq. (6), with the flowrate Q_w being driven by the piston, and the flowrate through the orifice Q_p being predicted via the numerical method outlined above. Figure 9 shows the comparison of the calculate powers (available to PTO) and the input power by the internal water surface. Then the power loss can be calculated as

$$R = \frac{\overline{P}_w - \overline{P}_p}{\overline{P}_w} \tag{23}$$

where the overbar means the time average value.

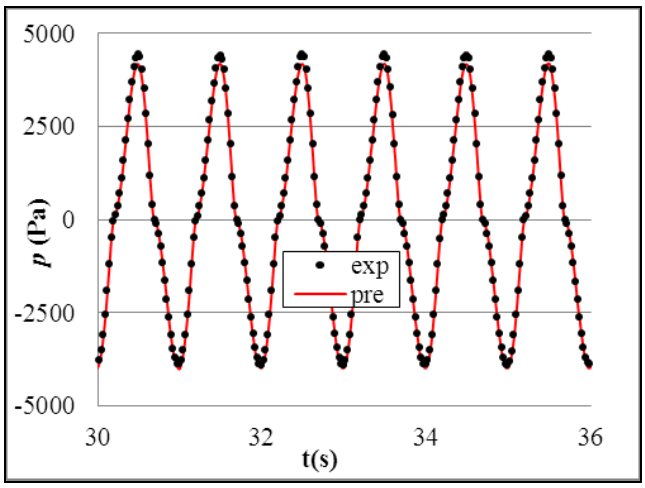

Figure 7 Measured and predicted chamber pressures

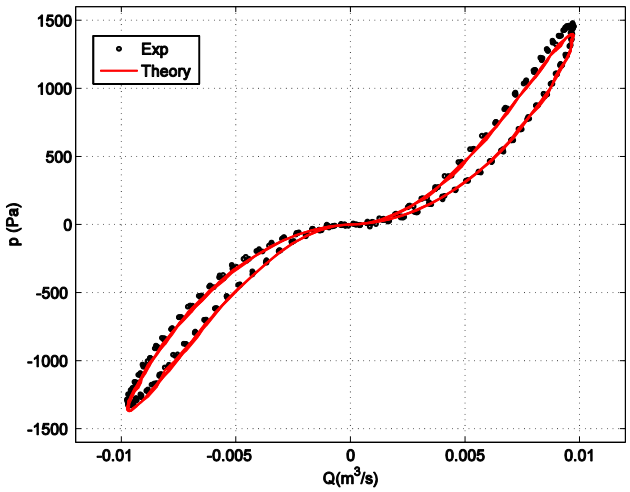

Figure 8 Comparison of the theoretical result and the measured data (A=0.045m, f=0.5Hz, ϕ=0.019m).

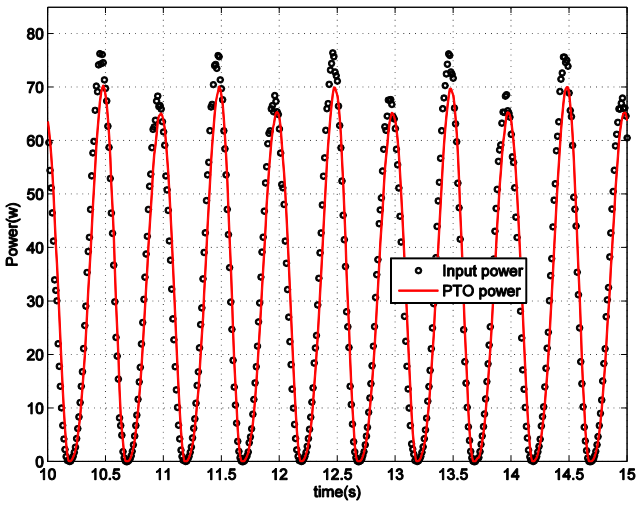

Figure 9 Power prediction for an orifice (A=0.045m, f=1.0Hz, ϕ=0.019m)

It is found that a small power loss is still seen from the calculation. Figure 9 shows a comparison of the time series of the input power given by the piston and the PTO power extracted by an orifice PTO. From the time series, it can be seen that there are some differences between the input power (provided by the piston) and the PTO power (which is available to the PTO system), especially at the negative peak of the pressure. The maximum difference of the powers can be about 10% in this case. However, detailed analysis has shown that the difference between the average input power and PTO power is much smaller than the appearance, which is only 0.52%. The reason for this is that when the air in the chamber is pressurized or de-pressurised, part of the input power is stored in the compressible air. When the chamber pressure returns from its positive or negative peaks, the stored power may be released. This is actually consistent with the assumption of isentropic process in the chamber. Generally the input power and the PTO power are similar, and a small difference between the input and the PTO powers can be seen, which can be regarded the power loss through the open boundary (the PTO system). It can be explained as when the air is pressurized and driven out of the chamber, its temperature is higher (thus internal energy is higher) than the atmosphere which is sucked into the chamber in the inhalation process. The difference between the internal energy of the exhaled and inhaled air is the power loss due to air compressibility in the air chamber. Obviously, the power loss will very much depend on the maximum chamber pressure and the flowrate.

VI. TIME-DOMAIN ANALYSIS

For an OWC wave energy converter, the application of the power take-off (PTO) system will damp the flow through the PTO and thus create pressurized and de-pressurised air in the chamber. For full scale OWC wave energy converter, the air compressibility may not be ignored due to the large air volume and chamber pressure (pressure gradient with regard to time). For such a system, regardless of the linear or nonlinear power take-off applied, the whole dynamic system is generally nonlinear, and thus a linear analysis is not enough.

In this study, a hybrid frequency-time domain approach has been adopted by combining the conventional potential flow analysis and the thermodynamics of the air flow outlined above. In the hydrodynamic analysis, the structure of the device is fixed as shown in Figure 1, and is identified as a rigid body (Body 1), whilst the water column (the so called piston) is the second rigid body (Body 2). In the WAMIT analysis, two-body system is applied, and the first body is fixed and the second body has only heave motion (Mode 9 in WAMIT analysis). The frequency domain analysis results are converted into the corresponding time-domain parameters, which in here are used for establishing a time-domain equation for the dynamic system.

In the formulation, due to the pressurised and de-pressurised air, in the time-domain equation for the piston motion, an additional force due to the chamber pressure is applied (see Eq. (24)), whilst the chamber pressure can be solved via the eqs. (21) and (22), with the chamber air volume formulation given by Eq. (25).

$$\left[M_{99}+A_{99}(\infty)\right]\ddot{x}_9+C_{99}x_9+b_{99}\dot{x}_9+\int_0^t K_{99}(t-\tau)\dot{x}_9(\tau)d\tau = F_9-A_0 p \tag{24}$$

where x_9 is the heave motion of the piston/water column (representing the internal water surface motion); M_{99} the mass of the piston/water column; $A_{99}(\infty)$ the corresponding added mass at the infinite frequency; b_1 the added viscous damping; C_{99} the restoring coefficient; K_{99} the retard function; F_9 the excitation force on the piston; p the chamber pressure; A_0 the sectional area of water column.

The chamber air volume can be calculated as

$$V = V_0 - A_0 x_9 \tag{25}$$

with V and V_0 being the air volumes of time-dependent and in calm water.

VII. RESULTS AND ANALYSIS

Solving the time-domain equation outlined above, we can obtain the chamber pressure responses (defined as the difference of the peak and the trough pressures divided by wave height H_w) and the IWS responses (defined as the difference of the IWS peak and trough motions divided by H_w) in regular waves under different orifices (therefore different damping from the PTO). Figure 10 and Figure 11 are the comparisons of the measured and predicted chamber pressure responses and the IWS responses for an orifice of 12mm in a wave height of about 40mm. Figure 12 and Figure 13 are the comparisons of the measured and predicted chamber pressure responses and the IWS responses for an orifice of 14mm in a wave height of about 40mm. From these comparisons, it can be seen that the numerical predictions proposed in the research have well predicted the chamber pressure and the internal water surface.

It must be emphasized that the dynamic system of the OWC device with nonlinear orifice PTOs is nonlinear, hence the responses presented for the nonlinear system are wave height dependent. In the numerical simulation, the wave heights are those measured from the tank tests. Though in the tank test, the wave heights are supposed to be a constant in a series regular wave tests, but the measured wave heights are normally different from those. For example, in the tank tests, the wave heights are supposed to be 40mm, but in reality the measured wave height are actually ranged from 38.4mm to 51.7mm, depending on the wave frequencies. This may be the reason why the numerical predictions are not very smooth.

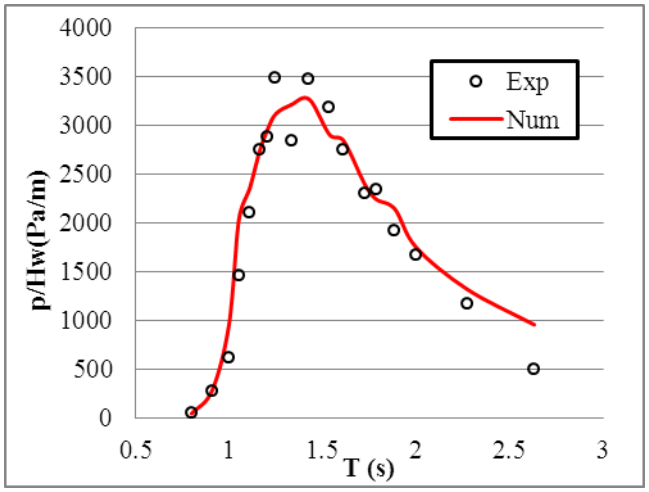

Figure 10 Responses of chamber pressure in regular waves (φ =12mm, H_w=40mm)

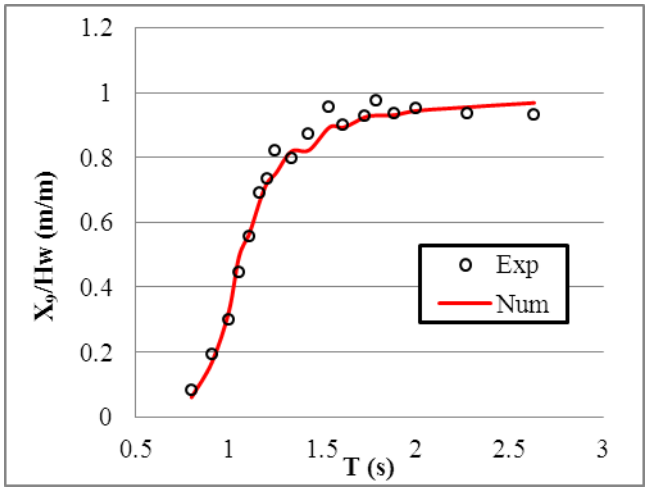

Figure 11 Responses of internal water surface in regular waves (φ =12mm, H_w=40mm)

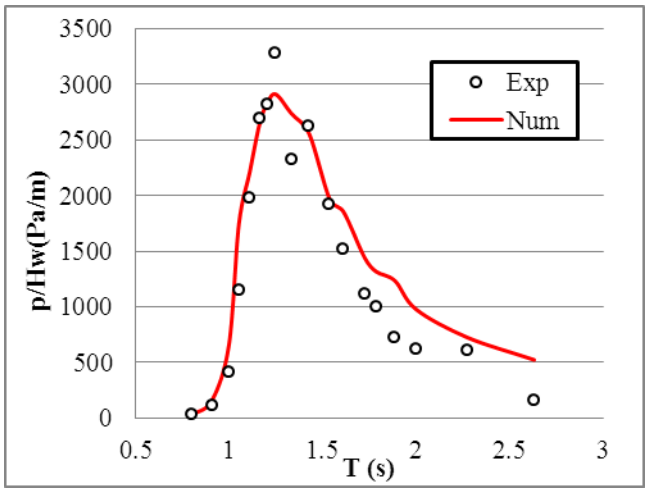

Figure 12 Responses of chamber pressure in regular waves (φ=14mm, H_w=40mm)

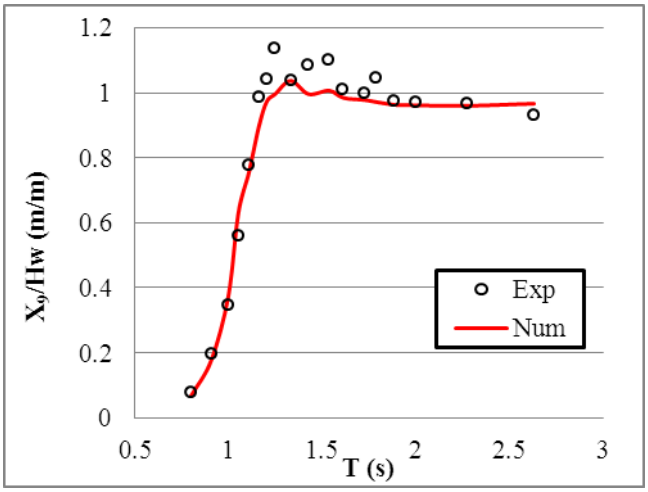

Figure 13 Responses of internal water surface in regular waves (φ =14mm, H_w=40mm)

VIII. CONCLUSIONS

In numerical simulations of OWC wave energy converters, the nonlinear effects, especially the nonlinear effects due to the nonlinear PTO and the relevant air compressibility, must be included, hence a hybrid time-domain analysis is often a convenient approach to solve the nonlinear dynamic problem and to assess the performance of the OWC devices in waves appropriately. By combining the potential flow analysis and the thermodynamics of the air flow in the air chamber, the time-domain equation for OWC wave energy converter has been formulated in this research. From the research and the examples given in this report, following conclusions can be drawn:

1) The comparisons between the experimental data and numerical simulation have shown the new method is very capable of assessing the OWC performance, including the chamber pressure responses and the internal water surface motion.
2) Though the example given in this research is for a fixed OWC wave energy converter, its principle can be used for floating OWC wave energy converter.
3) The internal water surface motion in the OWC device is represented by a piston, whose length is same as that of the water column.
4) The potential theory has well predicted the flow around the OWC device.

ACKNOWLEDGMENTS

This material is based upon works supported by the Science Foundation Ireland (SFI) under the Charles Parsons Award at Hydraulics and Maritime Research Centre (HMRC). Statistics and data were correct at the time of writing the article; however the authors wish to disclaim any responsibility for any inaccuracies that may arise.

REFERENCES

[1] Falcao, A., 2010, "Wave energy utilization: a review of the technologies," Renewable and Sustainable Energy Reviews, Vol. 14, pp. 899-918.
[2] Heath, T., 2012, "A review of oscillating water columns," Philosophical Transactions of the Royal Society A: Mathematical, Physical & Engineering Sciences, Vol. 370, pp. 235-245.
[3] Torre-Enciso, Y., Ortubia, I., Lopez de Aguileta, L. I. and Marques, J., 2009, "Mutriku Wave Power Plant: from the thinking out to the reality," Proceedings of the 8th European Wave and Tidal Energy Conference, Uppsala, Sweden, 7-10th Sep. 2009.
[4] EVE. Mutriku OWC Plant. cited: http://www.fp7-marinet.eu/EVE-mutriku-owc-plant.html (on: 27/03/2013).
[5] Sarmento, A. J. N. A. and Falcao, A. F. D. O., 1985, "Wave generation by an oscillating surface pressure and its application in wave-energy extraction," Journal of Fluid Mechanics, Vol. 150, pp. 467-485.
[6] Evans, D. V., 1982, "Wave-power absorption by systems of oscillating surface pressure distributions," Journal of Fluids Mechanics, Vol. 114, pp. 481-499.
[7] Evans, D. V. and Porter, R., 1995, "Hydrodynamic characteristics of an oscillating water column device," Applied Ocean Research, Vol. 17, pp. 155-164.
[8] Toyota, K., Nagata, S., Imai, Y. et al., 2010, "Primary energy conversion characteristics of a floating OWC 'Backward Bent Duct Buoy'," Proceedings of 20th International Offshore and Polar Engineering Conference, Beijing, China, 20-25 June, 2010.
[9] Imai, Y., Toyota, K., Nagata, S. et al., 2011, "An experimental study on generating efficiency of a wave energy converter 'Backward Bent Duct Buoy'," Proceedings of the 9th European Wave and Tidal Energy Conference, Southampton, UK, 5-9th Sep, 2011.
[10] Morris-Thomas, M. T., Irvin, R. J. and Thiagarajan, K. P., 2007, "An Investigation into the hydrodynamic efficiency of an oscillating water column," Journal of Offshore Mechanics and Arctic Engineering, Vol. 129, pp. 273-278.
[11] Sarmento, A. J. N. A., Gato, L. M. C. and de O. Falcao, A. F., 1990, "Turbine-controlled wave energy absorption by oscillating water column devices," Ocean Engineering, Vol. 17, pp. 481-497.
[12] Sheng, W., Alcorn, R. and Lewis, A., 2013, "On thermodynamics of primary energy conversion of OWC wave energy converters," Journal of Renewable and Sustainable Engineering, Vol. 5, doi: 10.1063/1.4794750
[13] Martins-rivas, H. and Mei, C.-C., 2009, "Wave power extraction from an oscillating water column along a straight coast," Ocean Engineering, Vol. 36, pp. 426-433.
[14] Mavrakos, S. A. and Konispoliatis, D. N. Hydrodynamic analysis of a vertical axisymmetric oscillating water column device floating in finite depth waters. Proceedings of the ASME 31st International Conference on Ocean, Offshore and Arctic Engineering, Rio de Janeiro, Brazil, July 1-6, 2012.
[15] WAMIT Inc, http://wamit.com/, cited on: 18/09/2011.
[16] ANSYS AQWA, http://www.ansys.com/Products/Other+Products/ANSYS+AQWA, cited on: 18/09/2011.
[17] Lee, C. H. and Nielsen, F. G., 1996, "Analysis of oscillating-water-column device using a panel method," International Workshop on Water Wave and Floating Bodies, Hamburg, Germany, 17-20, Mar. 1996.
[18] Evans, D. V., 1978, "The oscillating water column wave-energy device," IMA Journal of Applied Mathematics, Vol. 22, pp. 423-433.
[19] Evans, D. V., 1982, "Wave-power absorption by systems of oscillating surface pressure distributions," Journal of Fluid Mechanics, Vol. 114, pp. 481-499.
[20] Lee, C. H., Newman, J. N. and Nielsen, F. G., 1996, "Wave interaction with an oscillating water column," Proceedings of the 6th International Offshore and Polar Engineering Conference (ISOPE'96), Los Angeles, USA, May 26-31, 1996.
[21] Thakker, A. and Abdulhadi, R., 2008, "The performance of Wells turbine under bi-directional airflow," Renewable Energy, Vol. 33, pp. 2467-2474.

[22] Setoguchi, T., Santhakumar, S., Takao, M. et al., 2003, "A modified Wells turbine for wave energy conversion," Renewable Energy, Vol. 28, pp. 79-91.
[23] Falcao, A. F. d. O. and Justino, P. A. P., 1999, "OWC wave energy devices with air flow control," Ocean Engineering, Vol. 26, pp. 1275-1295.
[24] Thakker, A., Jarvis, J. and Sahed, A., 2009, "Design charts for impulse turbine wave energy extraction using experimental data," Renewable Energy, Vol. 34, pp. 2264-2270.
[25] Setoguchi, T., Santhakumar, S., Maeda, H. et al., 2001, "A review of impulse turbines for wave energy conversion," Renewable Energy, Vol. 23, pp. 261-292.
[26] Pereiras, B., Castro, F., Marjani, A. e. and Rodríguez, M. A., 2010, "An improved radial impulse turbine for OWC," Renewable Energy, Vol. 36, pp. 1477-1484.
[27] Kim, T., H., Setoguchi, T., Takao, M. et al., 2002, "Study of turbine with self-pitch-controlled blades for wave energy conversion," International Journal of Thermal Sciences, Vol. 41, pp. 101-107.
[28] Takao, M. and Setoguchi, T., 2012, "Air turbines for wave energy conversion," International Journal of Rotating Machinery, Vol. 2012, pp. doi:10.1155/2012/717398.
[29] Payne, G., "Guidelines for the experimental tank testing of wave energy converters," available: http://www.supergen-marine.org.uk/drupal/files/reports/WEC_tank_testing.pdf (10/01/2012).
[30] Lewis, A., Gilbaud, T. and Holmes, B., 2003, "Modelling the Backward Bent Duct Device-B2D2, a comparison between physical and numerical models," Proceedings of 5th European Wave Energy Conference, Cork, Ireland, 17-20th, Sep. 2003.
[31] Forestier, J. M., Holmes, B., Barret, S. and Lewis, A., 2007, "Value and validation of small scale physical model tests of floating wave energy converters," Proceedings of the 7th European Wave and Tidal Energy Conference, Porto, Portugal, 11-14th Sep. 2007.
[32] Sheng, W., Brian, F., Lewis, A. W. and Alcorn, R., 2012, Experimental studies of a floating cylindrical OWC WEC,
[33] Toyota, K., Nagata, S., Imai, Y. and Setoguchi, T., 2008, "Effects of hull shape on primary conversion characteristics of a floating OWC 'Backward Bent Duct Buoy'," Journal of Fluid Science and Technology, Vol. 3, pp. 458-465.
[34] Sheng, W., Brian, F., Lewis, A. W. and Alcorn, R., 2012, "Experimental studies of a floating cylindrical OWC WEC," Proceedings of OMAE 2012 Conference, Rio de Janeiro, 1-6th July, 2012.
[35] Sarmento, A., Gato, L. M. C. and Falcao, A., 1990, "Turbine-controlled wave energy absorption by oscillating water column devices," Ocean Engineering, Vol. 17, pp. 481-497.
[36] Thakker, A., Dhanasekaran, T. S., Takao, M. and Setoguchi, T., 2003, "Effects of compressibility on the performance of a wave-energy conversion device with an impulse turbine using a numerical simulation technique," International Journal of Rotating Machinery, Vol. 9, pp. 443–450.